

# 3-dimensional fiber Bragg grating strain and displacement sensing system based on a cylinder structure

Jianhua LUO, Bo LIU (✉), Yuwen LAN, Shuzhong YUAN, Guiyun KAI, Xiaoyi DONG

Institute of Modern Optics, Key Laboratory of Photoelectric Information Technical Science, Nankai University, Tianjin 300071, China

© Higher Education Press and Springer-Verlag 2008

**Abstract** A novel 3-dimensional fiber Bragg grating (FBG) strain and displacement sensing system based on a cylinder structure was proposed. Three FBGs, fixed in the outer surface of the cylinder at the same level according to a  $120^\circ$  angle interval, were used as sensing elements. In principle, the three FBGs have some fixed relationship when a strain  $F$  is put on the cylinder. Based on the principles of physics and mathematics, theoretical derivations and the experimental set-up were shown. According to the experimental results, this sensor could measure the size and angles of the strain or displacement accurately.

**Keywords** frequency splitting, distributed Bragg reflector (DBR) fiber laser, lateral pressure

## 1 Introduction

Fiber Bragg grating (FBG), as a novel sensing element, has attractively progressed, outperforming conventional sensors with its high sensitivity, fast response, low cost, light weight, and immunity to electromagnetic interference [1]. During the past 20 years, various FBG-type sensors used for different requirements have emerged with their applied fields expanding rapidly. The precise measurements of strain, displacement, torsion angle, torque, electric current, temperature, gas, and other quantities have been realized [2–10]. In practice, the sensing system is given much attention [11–13]. Multi-dimensional and multi-parameter measurements are necessary. Reference [14] reported a triaxial Bragg grating accelerometer and demonstrated the operation of the prototype of the proposed triaxial accelerometer with only one active direction.

In this paper, a novel 3-dimensional FBG strain and displacement sensing system based on a cylindrical structure, which can measure the size and direction of the strain or displacement by measuring wavelength shifts of the

three FBGs, was proposed. Compared with normal FBG sensors, this sensing system was capable of measuring strain from any direction. In addition, with strain  $F$  and the size of cylinder, its displacement could also be deduced simultaneously. Based on the principles of physics and mathematics, calculation of the system design and function were also shown.

## 2 Theory

The basic principle of the operation commonly used in an FBG-based sensor system is to monitor the shifts in wavelength of the returned “Bragg” signal with the changes in the measured parameters such as strain and temperature. The Bragg wavelength, or resonance condition of a grating, can be expressed as

$$\lambda = 2n_{\text{eff}}\Lambda, \quad (1)$$

where  $\lambda$  is the resonance wavelength, and  $\Lambda$  and  $n_{\text{eff}}$  are the grating period and the effective index of the core, respectively.

Due to the photo-elastic effects and the thermal response, the shift in the resonance wavelength with strain and temperature can be expressed as

$$\Delta\lambda = \lambda_0(K_T\Delta T + K_\varepsilon\varepsilon), \quad (2)$$

where  $\Delta T$  and  $\varepsilon$  are the changes in temperature and strain; the coefficients  $K_T$  and  $K_\varepsilon$  are the temperature and strain sensitivities of the resonance wavelength shift ( $\Delta\lambda$ ), respectively; and  $\lambda_0$  is the initial resonance wavelength.

When there is no change in temperature, the resonance wavelength shift ( $\Delta\lambda$ ) would be determined only by  $\varepsilon$ . In this paper, since the environment temperature is supposed to be stable,

$$\Delta\lambda = \lambda_0K_\varepsilon\varepsilon = \lambda_0(1 - P_e)\varepsilon, \quad (3)$$

where  $P_e$  is the effective photoelastic coefficient.

As shown in Fig. 1, three FBGs are fixed on the side of the cylinder at  $120^\circ$  angle intervals. When the FBG length is significantly less than  $L$ , the cylinder length, it is supposed that the three FBGs are fixed in one circular section. If a strain  $F$  is on the cylinder, the FBGs would get a different strain. Thus, the size and direction of  $F$  could be deduced by measuring the strain on the three FBGs. Meanwhile, the strains on the three FBGs could be obtained by measuring the shifts of their wavelengths.

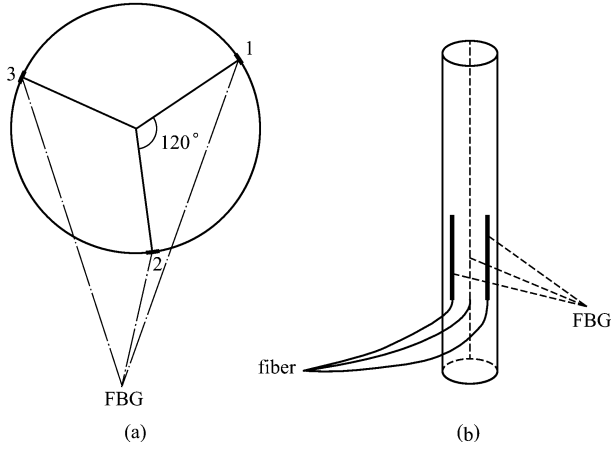


Fig. 1 Cylinder sensor. (a) Sectional diagram; (b) cylinder

As shown in Fig. 2, the cylindrical coordinate system was used for analysis. The circular section where the three FBGs are located was taken as the axis plane, and one of the FBG directions as the  $x$ -axis.  $l$  is the distance  $x$ -axis to the free end and  $r$  is the cylinder radii. All parameters were marked out in the diagram. According to rigid body mechanics, the following equations could be obtained:

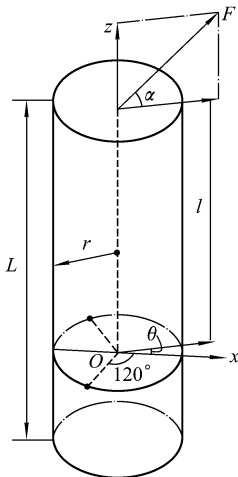


Fig. 2 Schematic plan of sensor

$$\begin{cases} \varepsilon_1 = -\frac{F \cos \alpha \times l \times \cos \theta}{IE} + \frac{F \sin \alpha}{\pi r^2 E} = \frac{\Delta \lambda_1}{\lambda_{10}(1-P_e)}, \\ \varepsilon_2 = -\frac{F \cos \alpha \times l \times \cos\left(\frac{4\pi}{3} - \theta\right)}{IE} + \frac{F \sin \alpha}{\pi r^2 E} = \frac{\Delta \lambda_2}{\lambda_{20}(1-P_e)}, \\ \varepsilon_3 = -\frac{F \cos \alpha \times l \times \cos\left(\frac{2\pi}{3} - \theta\right)}{IE} + \frac{F \sin \alpha}{\pi r^2 E} = \frac{\Delta \lambda_3}{\lambda_{30}(1-P_e)}, \end{cases} \quad (4)$$

where  $E$  and  $I$  are the elastic modulus and moment of the inertia of cylinder, respectively.  $I$  can be expressed by  $I = \pi r^4/4$ .

According to the formulas above, it can be deduced that

$$\begin{cases} \lambda_i = \lambda_{i0} + M_i F, \quad i = 1, 2, 3, \\ M_1 = \lambda_{10} K_\varepsilon \left( -\frac{\cos \alpha \times l \times \cos \theta}{IE} + \frac{\sin \alpha}{\pi r^2 E} \right), \\ M_2 = \lambda_{20} K_\varepsilon \left( -\frac{\cos \alpha \times l \times \cos\left(\frac{4\pi}{3} - \theta\right)}{IE} + \frac{\sin \alpha}{\pi r^2 E} \right), \\ M_3 = \lambda_{30} K_\varepsilon \left( -\frac{\cos \alpha \times l \times \cos\left(\frac{2\pi}{3} - \theta\right)}{IE} + \frac{\sin \alpha}{\pi r^2 E} \right). \end{cases} \quad (5)$$

Once a strain  $F$  was put on the sensor, all the angles and the rate of slope  $M$  would be determined. Therefore, it can be concluded that the wavelength  $\lambda$  is in direct proportion to strain  $F$ . With all the known quantities, Eq. (5) could be solved and all the variables ( $F$ ,  $\theta$ ,  $\alpha$ ) could also be deduced.

On the other hand, according to rigid body mechanics, it can also be inferred that when strain  $F$  was put on the cylinder perpendicularly, the deflection, namely the lateral displacement, at the free end of the cylinder could be obtained as  $S_{xy} = FL^3/(3IE)$ ; when  $F$  was parallel to the cylinder, the tensile would be  $S_z = \varepsilon_z L = FL/(\pi r^2 E)$ . Thus, the whole displacement would be  $S = (S_{xy}^2 + S_z^2)^{1/2}$ .

### 3 Experiment and results

In this experiment, the cylinder bottom was fixed and the top was set to be variable. Strain  $F$  was put on the top by using a 3-dimensional fixed pulley system. When weight was put on the cylinder, all FBGs would have wavelength shifts. The weight on the cylinder could be then deduced by measuring the shifts.

The experimental facility is shown in Fig. 3. A broadband source of light form reached the 3-dimensional FBG sensor and was reflected to a spectrometer via 3 dB

coupler. The spectrometer was used to memorize the shifts of the FBG wavelengths. An optical switch was also used to link the three FBGs. In this experiment, the FBG was fabricated by phase mask method, and their center wavelengths in free were 1560.1, 1558.6 and 1558.9 nm, respectively. The cylinder was made by Perspex.

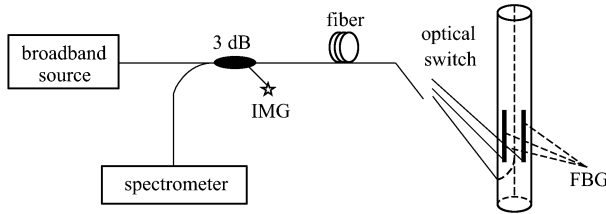


Fig. 3 Experimental setup (IMG: index matching glue)

Based on experimental data, the fitting curves are given in Fig. 4, which illustrates the relationship between  $F$  and wavelength. From Fig. 4, it can be found that all the fitting curves were linear with a very high linearity, corresponding with our theoretical derivations. With the curves' fitting equations, the measured value  $F'$  could be deduced. Table 1 compares the measured with the actual value  $F$ , its deviation and standard deviation. It can be seen that these two group values match very well. The max standard error is 0.026041. In addition, the angles (i.e.,  $\alpha$ ,  $\theta$ ) could be deduced using the rate of slope  $M$  shown in Eq. (6), so as the displacement of the cylinder. All the results are shown in Table 1, where the length of cylinder,  $L$ , is 0.2 m.

$$\left\{ \begin{aligned} \tan \theta &= -\sqrt{3} \cdot \frac{\frac{M_2}{\lambda_{20}} - \frac{M_3}{\lambda_{30}}}{2 \frac{M_1}{\lambda_{10}} - \frac{M_2}{\lambda_{20}} - \frac{M_3}{\lambda_{30}}} = -1.119819949, \\ \tan \alpha &= -\frac{4l \cos \theta}{r} \cdot \frac{\frac{M_1}{\lambda_{10}} + \frac{M_2}{\lambda_{20}} + \frac{M_3}{\lambda_{30}}}{2 \frac{M_1}{\lambda_{10}} - \frac{M_2}{\lambda_{20}} - \frac{M_3}{\lambda_{30}}} = -1.939499178. \end{aligned} \right. \quad (6)$$

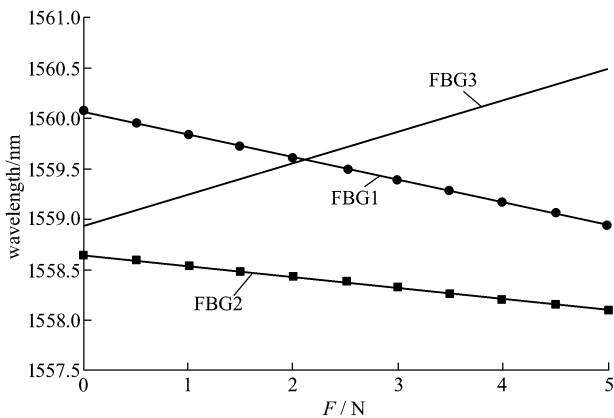


Fig. 4 Fitting curves of wavelength as a function of strain  $F$  (FBG1:  $\{y\}_N = -0.2232\{x\}_N + 1560.1$ ,  $R^2 = 0.9995$ ; FBG2:  $\{y\}_N = -0.1086\{x\}_N + 1558.6$ ,  $R^2 = 0.9998$ ; FBG3:  $\{y\}_N = 0.3099\{x\}_N + 1558.9$ ,  $R^2 = 0.9995$ )

Table 1 Experimental data

$F'/N$	$F/N$	$F' - F/N$	standard deviation	$S_x/\mu\text{m}$	$S_z/\mu\text{m}$	$S/\mu\text{m}$
0.036827	0.0	0.036827	0.026041	6.29	-0.028	6.29
0.485687	0.5	-0.014313	0.010121	83.00	-0.370	83.00
0.974897	1.0	-0.025103	0.017751	167.00	-0.740	167.00
1.491955	1.5	-0.008045	0.005689	255.00	-1.100	255.00
1.988447	2.0	-0.011553	0.008169	340.00	-1.500	340.00
2.507414	2.5	0.007414	0.005242	428.00	-1.900	428.00
3.012227	3.0	0.012227	0.008646	515.00	-2.300	515.00
3.503135	3.5	0.003135	0.002217	599.00	-2.700	599.00
4.016887	4.0	0.016887	0.011941	686.00	-3.100	686.00
4.480380	4.5	-0.019620	0.013873	766.00	-3.400	766.00
5.002024	5.0	0.002024	0.001431	855.00	-3.800	855.00

From Eq. (6), it can be deduced that  $\theta \approx 311.76^\circ$  and  $\alpha \approx -62.72^\circ$ .

### 4 Conclusions

In this paper, a novel FBG sensing system based on a cylindrical structure is proposed. Compared with normal FBG sensors, this sensing system is capable of simultaneous 3-dimensional measurement of strain and displacement. In addition, due to its applicability for wavelength division multiplexing (WDM) systems, sensing networks can be constructed using FBG sensors to realize multi-dimensional and multi-parameter measurements. The sensing system shows good potential for smart sensing.

**Acknowledgements** The project was supported by the National High Technology Research and Development Program of China (Grant No. 2006AA01Z217), the National Natural Science Foundation of China (Grant No. 60736039) and the Key Laboratory Fund of Optoelectronic Information Technical Science, Ministry of Education of China.

### References

1. Kersey A D, Davis M A, Patrick H J, et al. Fiber grating sensors. *Journal of Lightwave Technology*, 1997, 15(8): 1442–1463
2. Zhang J Z, Peng G D, Yuan L, et al. Simultaneous long- and short-gauge strain measurement in spectral domain by a novel optical fiber sensor unit. *IEEE Photonics Technology Letters*, 2007, 19(14): 1084–1086
3. Xue L F, Liu J G, Liu Y G, et al. Method for enhancing temperature sensitivity of fiber Bragg gratings based on bimetallic sheets. *Applied Optics*, 2006, 45(31): 8132–8135
4. Lee B. Review of the present status of optical fiber sensors. *Optical Fiber Technology*, 2003, 9(2): 57–79
5. Guo T, Zhao Q D, Zhang H, et al. Temperature-insensitive fiber Bragg grating dynamic pressure sensing system. *Optics Letters*, 2006, 31(15): 2269–2271
6. Zhao C L, Demokan M S, Jin W, et al. A cheap and practical FBG temperature sensor utilizing a long-period grating in a photonic crystal fiber. *Optics Communications*, 2007, 276(2): 242–245

7. Zhang W T, Li F, Liu Y L, et al. Ultrathin FBG pressure sensor with enhanced responsivity. *IEEE Photonics Technology Letters*, 2007, 19(19): 1553–1555
8. Shao L Y, Dong X Y, Zhang A P, et al. High-resolution strain and temperature sensor based on distributed Bragg reflector fiber laser. *IEEE Photonics Technology Letters*, 2007, 19(20): 1598–1600
9. Yang J, Zhao Y, Yang S Y, et al. A micro-vibration measurement method based on Isostrain cantilever and cascade self-demodulated FBG pair. *Sensor Letters*, 2007, 5(2): 361–365
10. Li H N, Zhou G D, Ren L, et al. Strain transfer analysis of embedded fiber Bragg grating sensor under nonaxial stress. *Optical Engineering*, 2007, 46(5): 054402
11. Liu S C, Yu Y L, Zhang J T, et al. Real-time monitoring sensor system for fiber Bragg grating array. *IEEE Photonics Technology Letters*, 2007, 19(19): 1493–1495
12. Su H, Huang X G. A novel fiber Bragg grating interrogating sensor system based on AWG demultiplexing. *Optics Communications*, 2007, 275(1): 196–200
13. Liu D, Ngo N Q, Tjin S C, et al. A dual-wavelength fiber laser sensor system for measurement of temperature and strain. *IEEE Photonics Technology Letters*, 2007, 19(15): 1148–1150
14. Morikawa S R K, Ribeiro A S, Regazzi R D, et al. Triaxial Bragg grating accelerometer. In: : *Proceedings of the 15th Optical Fiber Sensors Conference Technical Digest*, 2002, 1: 95–98